Forcing associated with contrail dehydration and soot emissions in a global climate model

Joyce Penner

Presented at the 5th UTIAS International Workshop on Aviation and Climate Change

Toronto, May 18-20, 2015

(Published in Schumann et al., ACP, 2016)

Effects of aircraft soot emissions:

- Direct forcing (small)
- Linear contrail formation
- Spreading contrails ("contrail cirrus") and resulting atmospheric "deyhydration"
- Effects of soot emissions on large scale cirrus clouds

Questions regarding contrail dehydration

- Can we simulate contrails from a large number of aircraft flights in a global climate model consistent with observations?
- How does exchange of humidity between contrails and ambient air change contrail properties?
- How strongly do contrails change the atmosphere by dehydration/hydration?
- Can we quantify the radiative impact of contrail-induced dehydration/hydration?

Sedimenting fall streaks have been observed

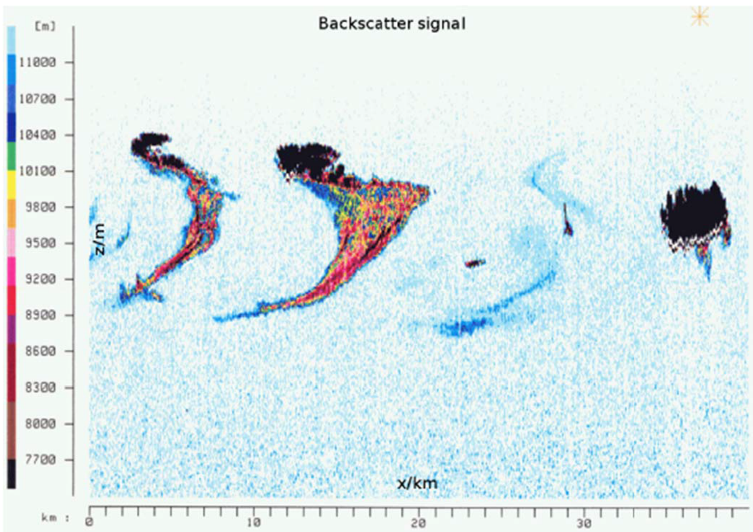

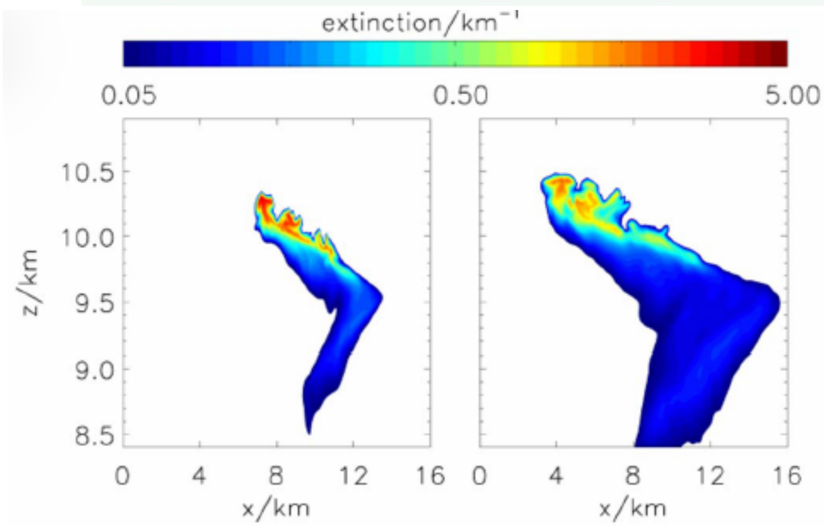

- Vertical cross-section of (airborne downward looking) Lidar backscatter with multiple fallstreaks from sedimenting contrails (scale: 2 x 5 km) (Schumann, 1994)

- LES Extrinction fields (right) after 2 and 3 h, show similar fallstreaks (Unterstrasser et al., 2012)

Method

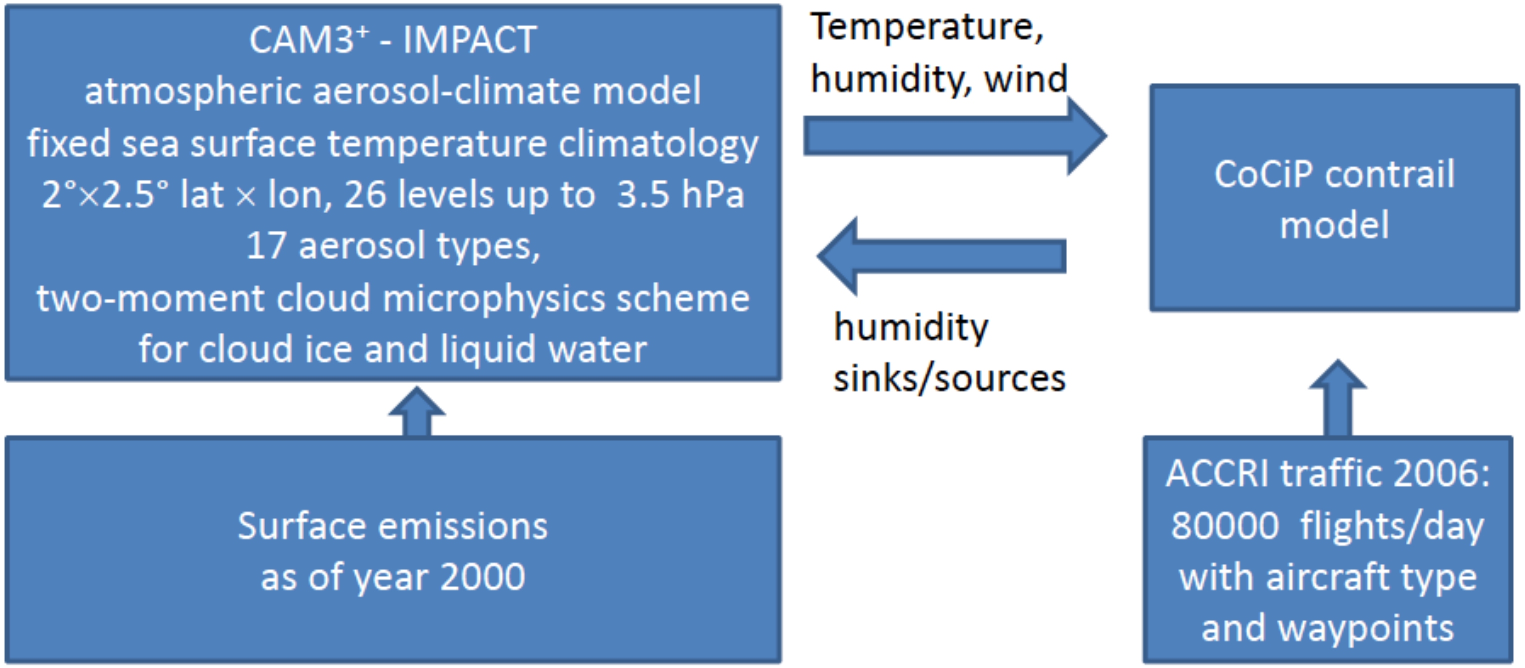

Table 1. Schematic run specification

Run	Coupling method	Emission amounts	Integration period
0	offline	nominal	30 years
1	online	nominal	30 years
2	online	100 × increased	1 year

Contrail processes approximated in CoCiP

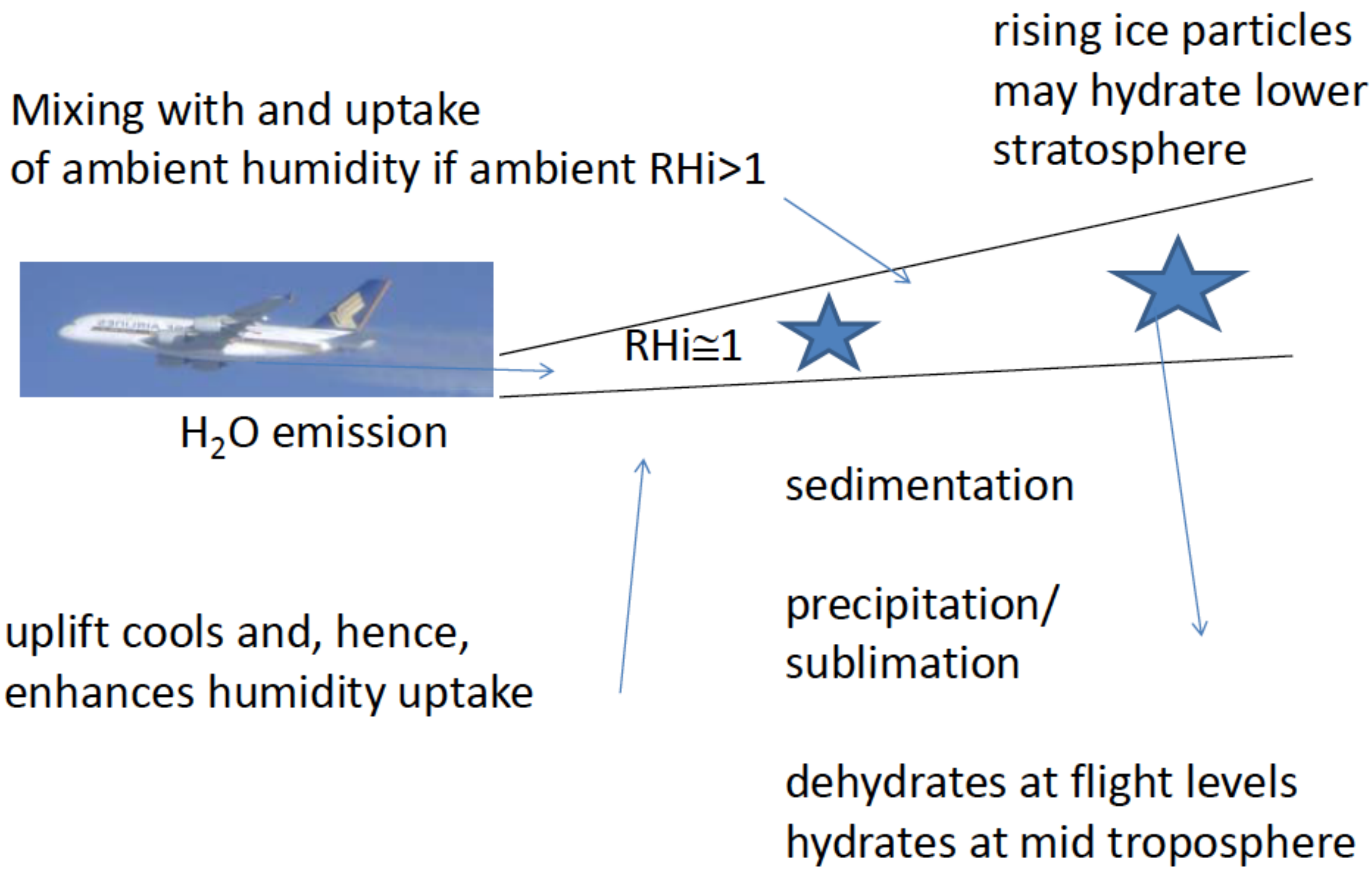

Exchange of H_2O between aircraft, contrails and atmosphere in CAM3+/IMPACT/CoCiP

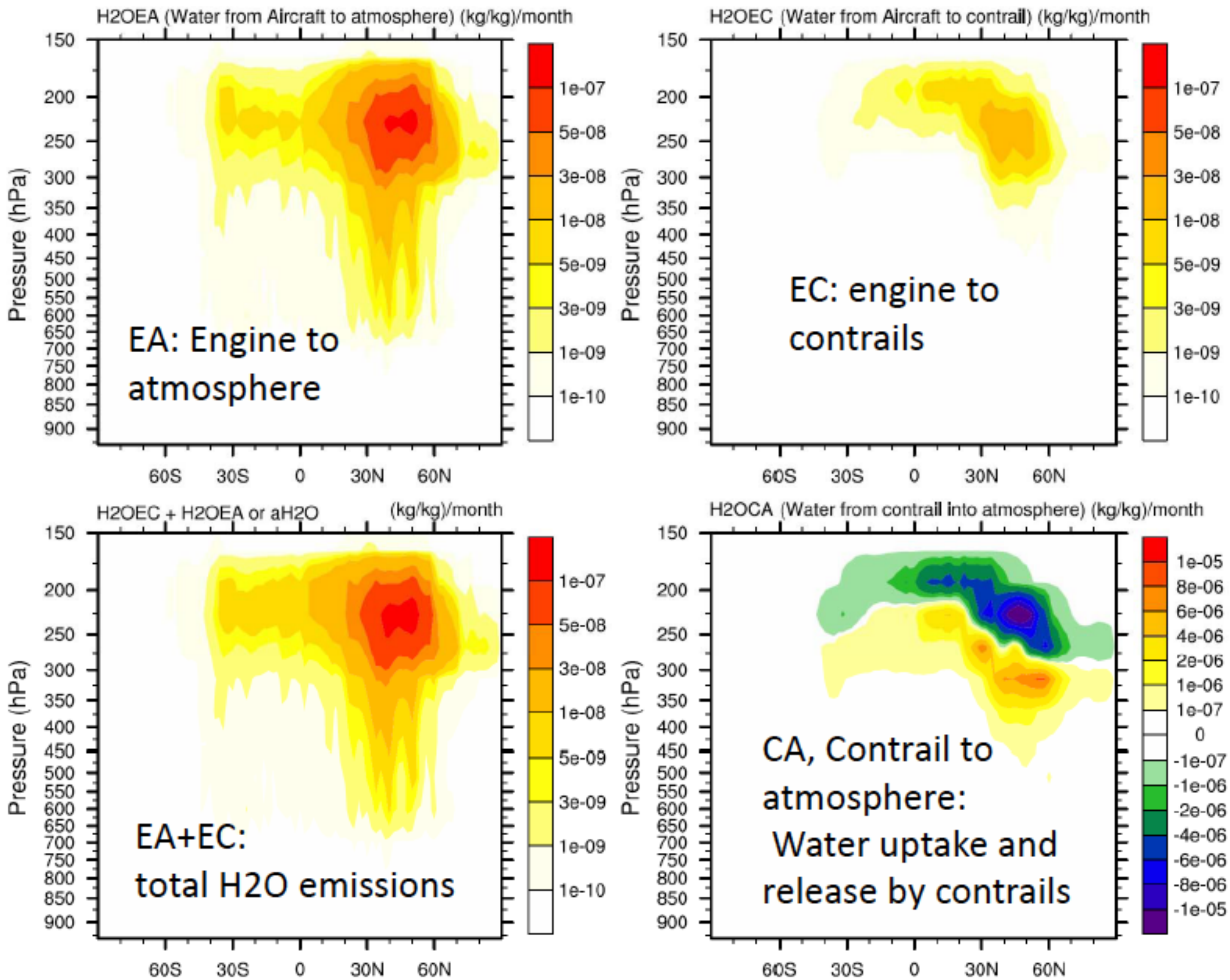

Results

- Global maps of contrail properties
- Basic impact of coupling on contrails: reduced water content
- Comparison of contrail properties with observations, theory, and simulation results
- Can we see a systematic dehydration effect in the noisy global model results (CAM)?
- Estimates for 100 * increased traffic emissions

- Run 1
- Global mean cirrus cover (top)

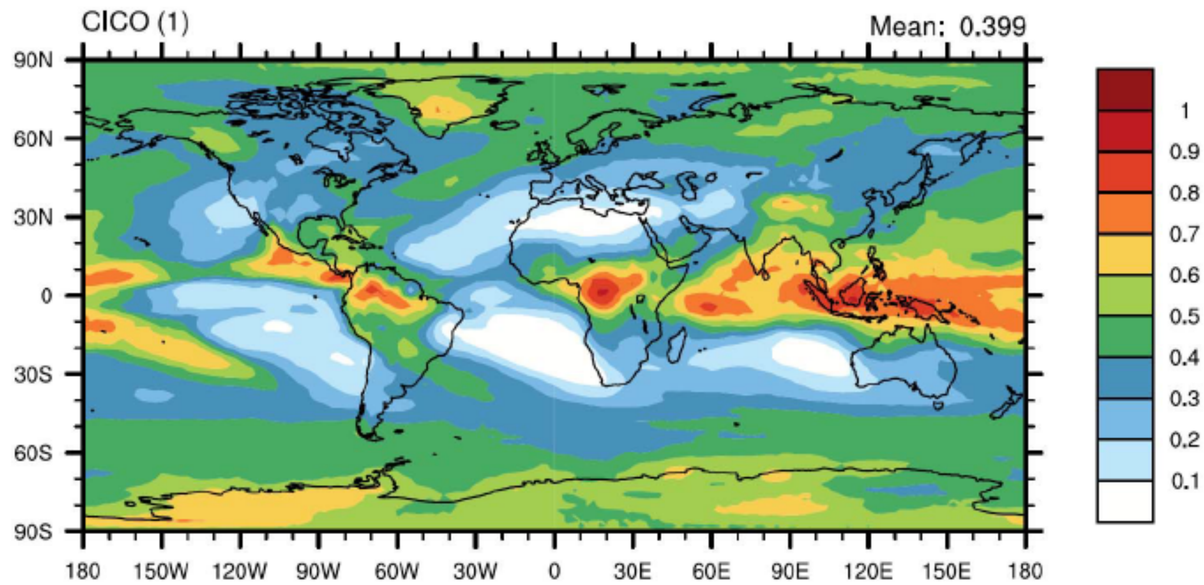

- Cover of contrails exceeding optical depth 0.1 (bottom)

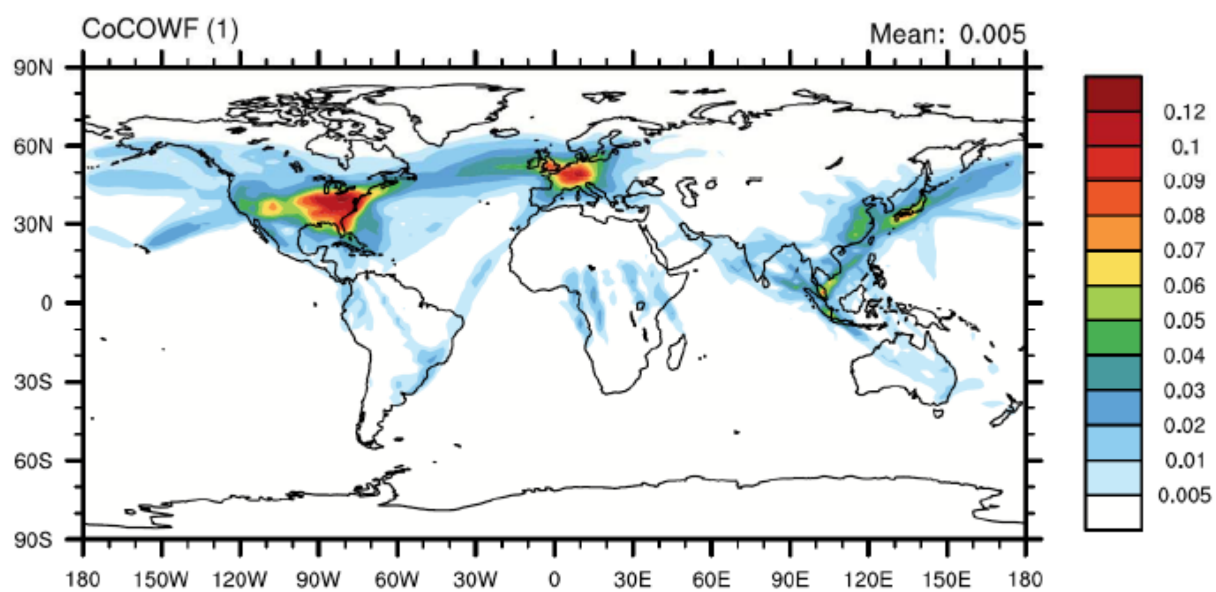

- Run 1 – Run 0
- Annual mean radiative forcing by contrails
- The net RF, not shown is 0.061 W/m^2, and is non-negative everywhere

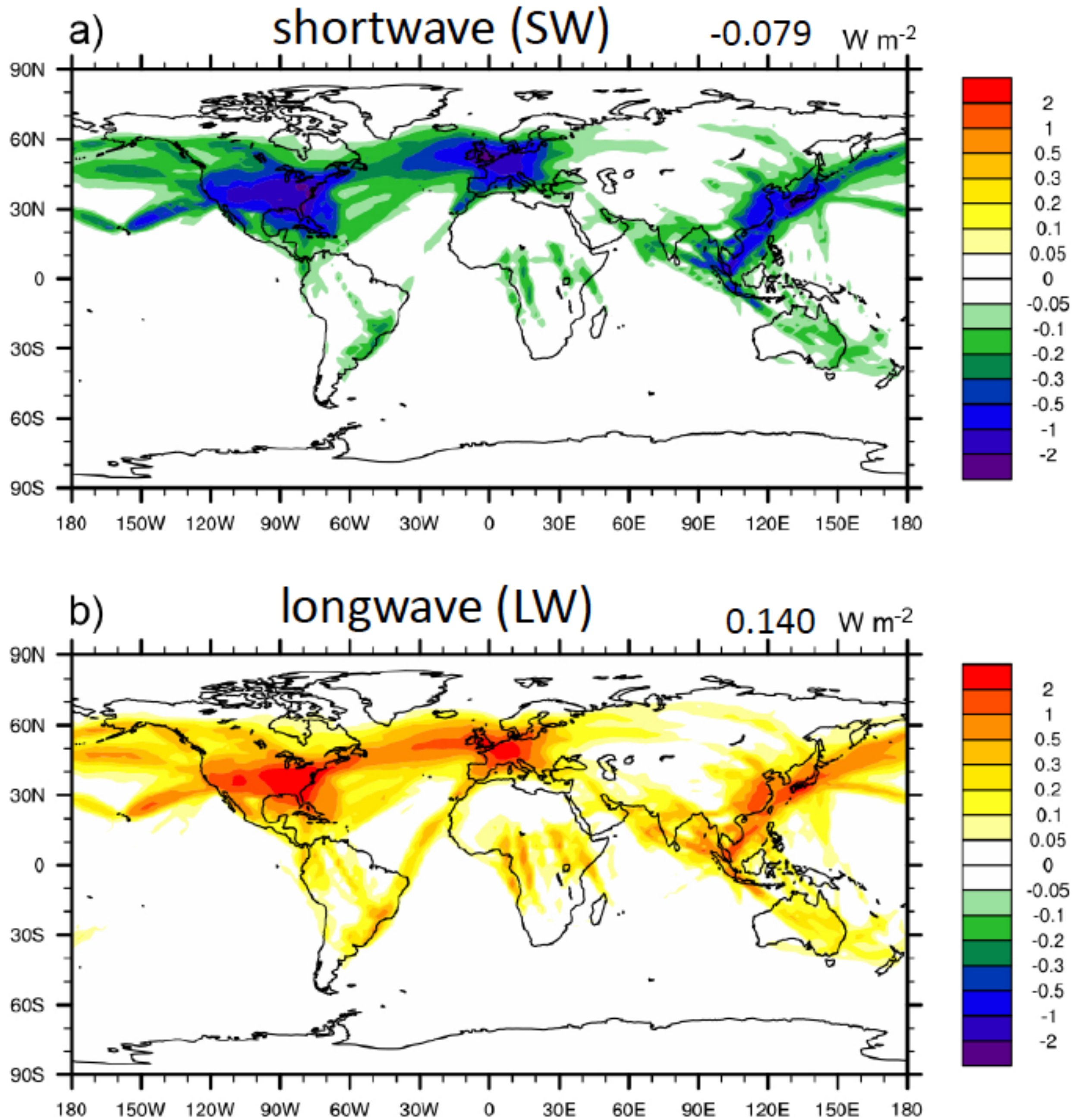

?

Coupling reduces RHi

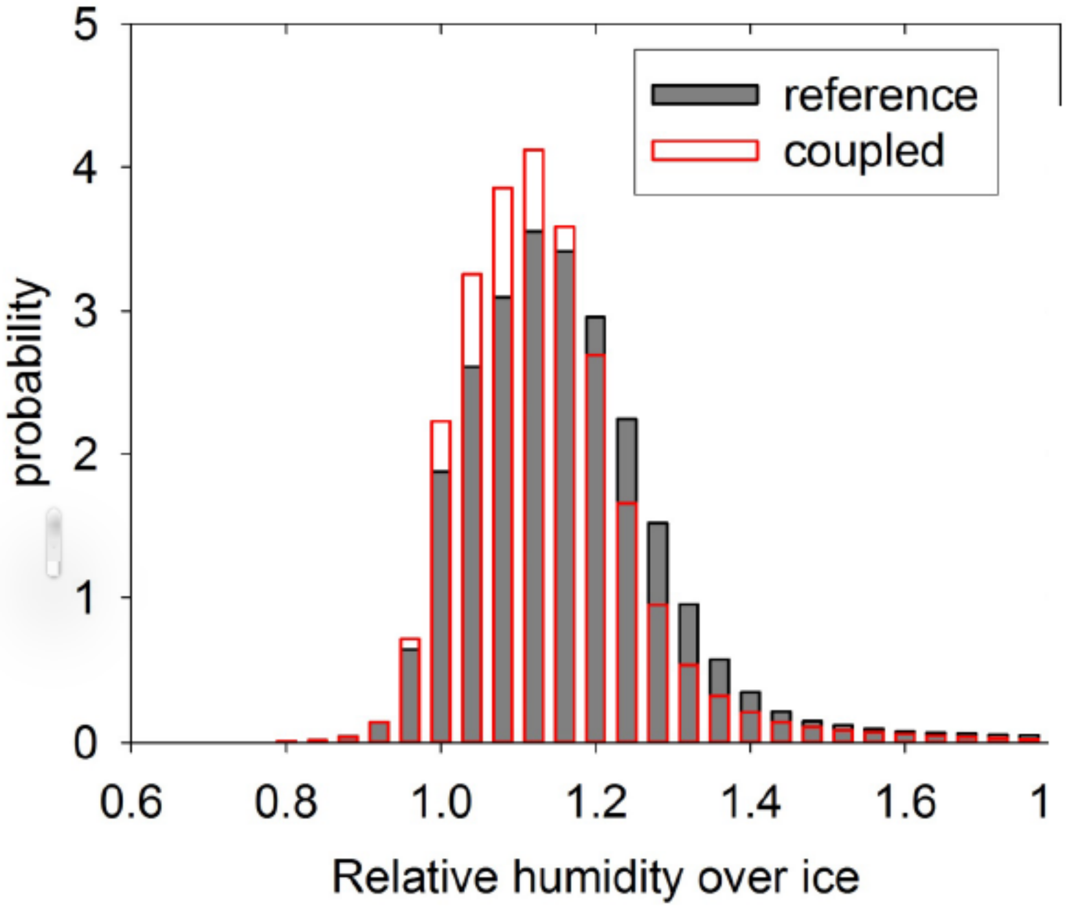

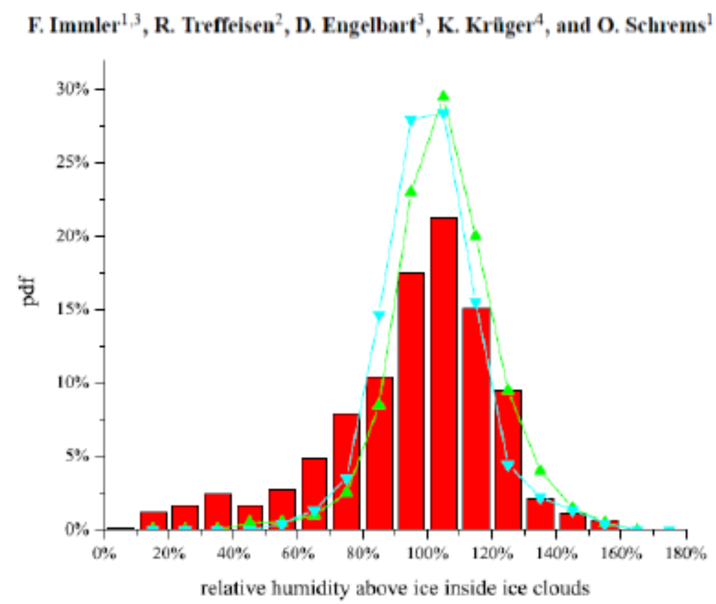

Fig. 4. PDF of the relative humidity above ice measured by radiosondes in the altitude ranges where the lidar detected cirrus clouds. For comparison, in situ measurements from the INCA campaigns (Northern Hemisphere: green, Southern Hemisphere: cyan) are shown (Ovarlez et al., 2002).

Coupling increases age slightly

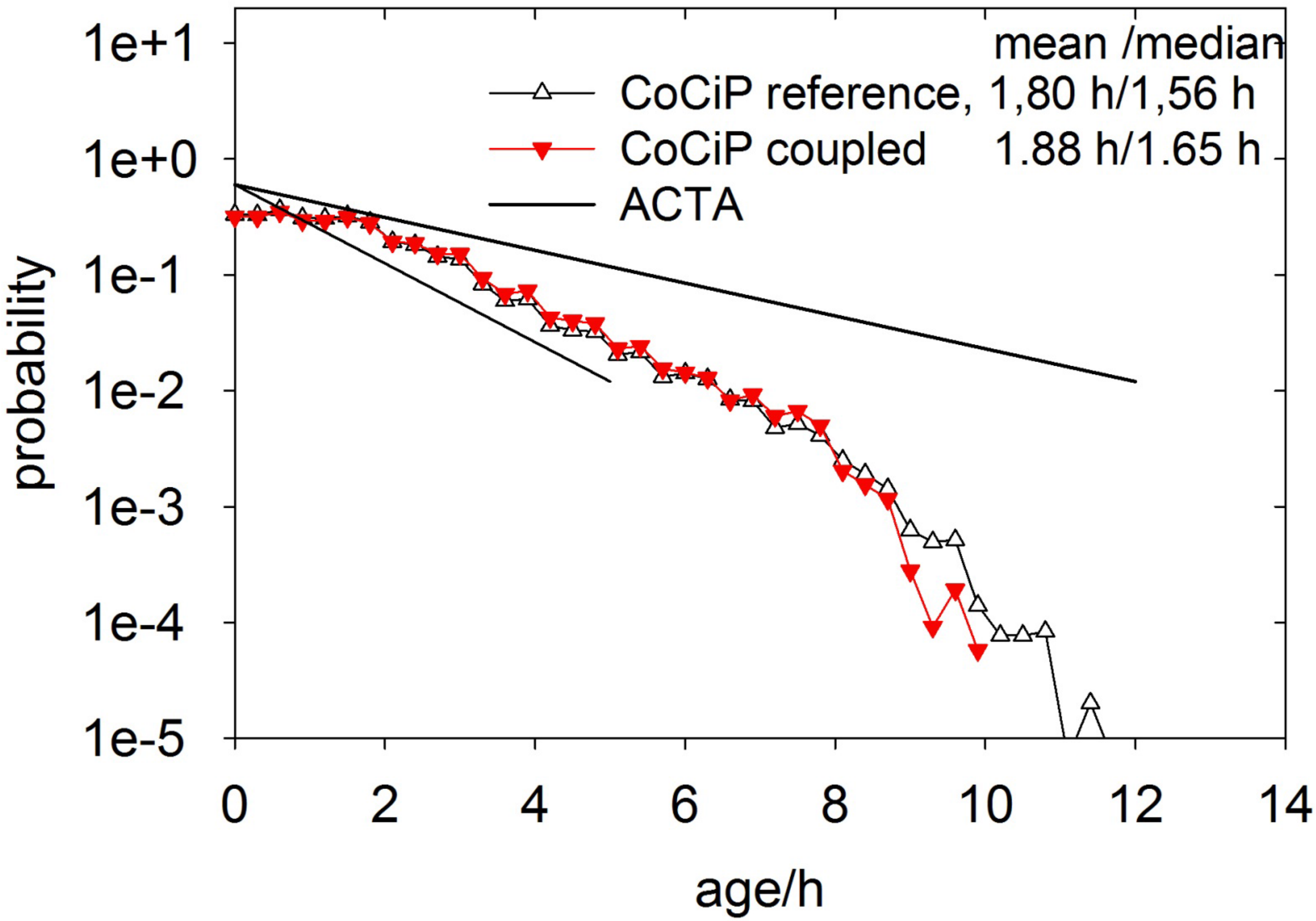

ACTA: upper and lower bounds of contrails tracked with the ACTA algorithm in infrared Meteosat data (Vazquez-Navarro et al., 2015)

Pdf of solar optical depth occurrence

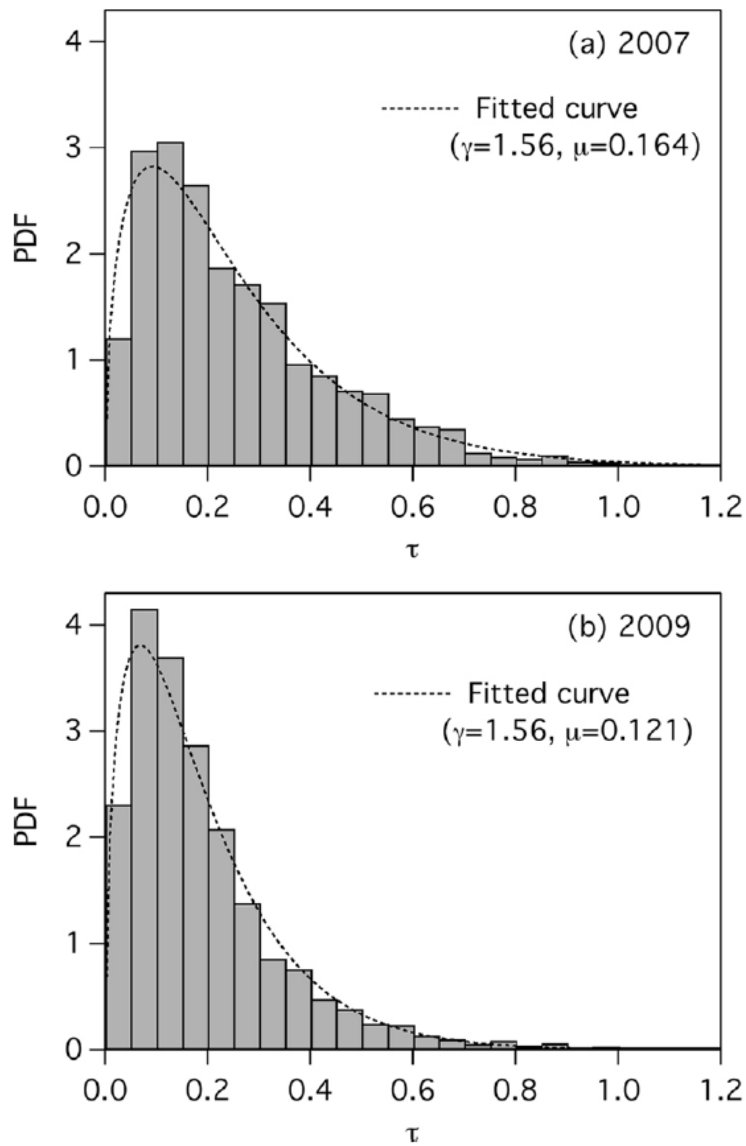

MODIS-CALIPSO, Iwabuchi et al., 2012

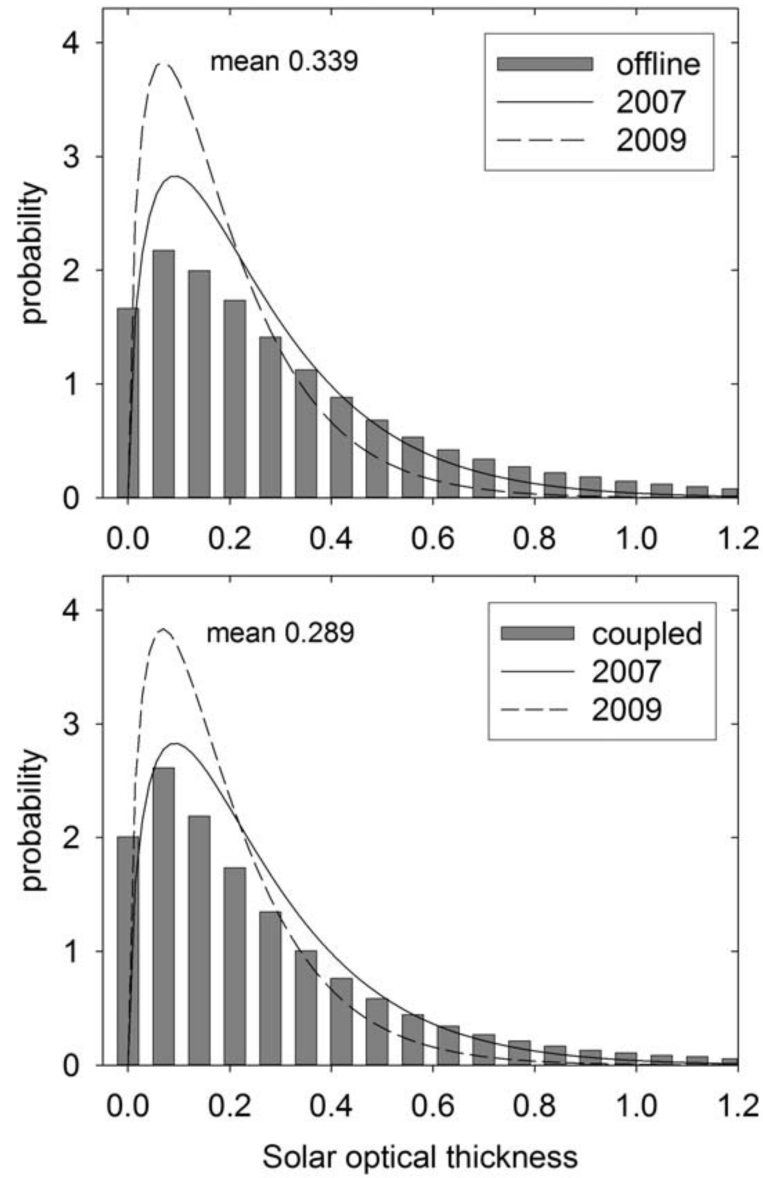

CoCiP-CAM, with curves from Iwabuchi et al.

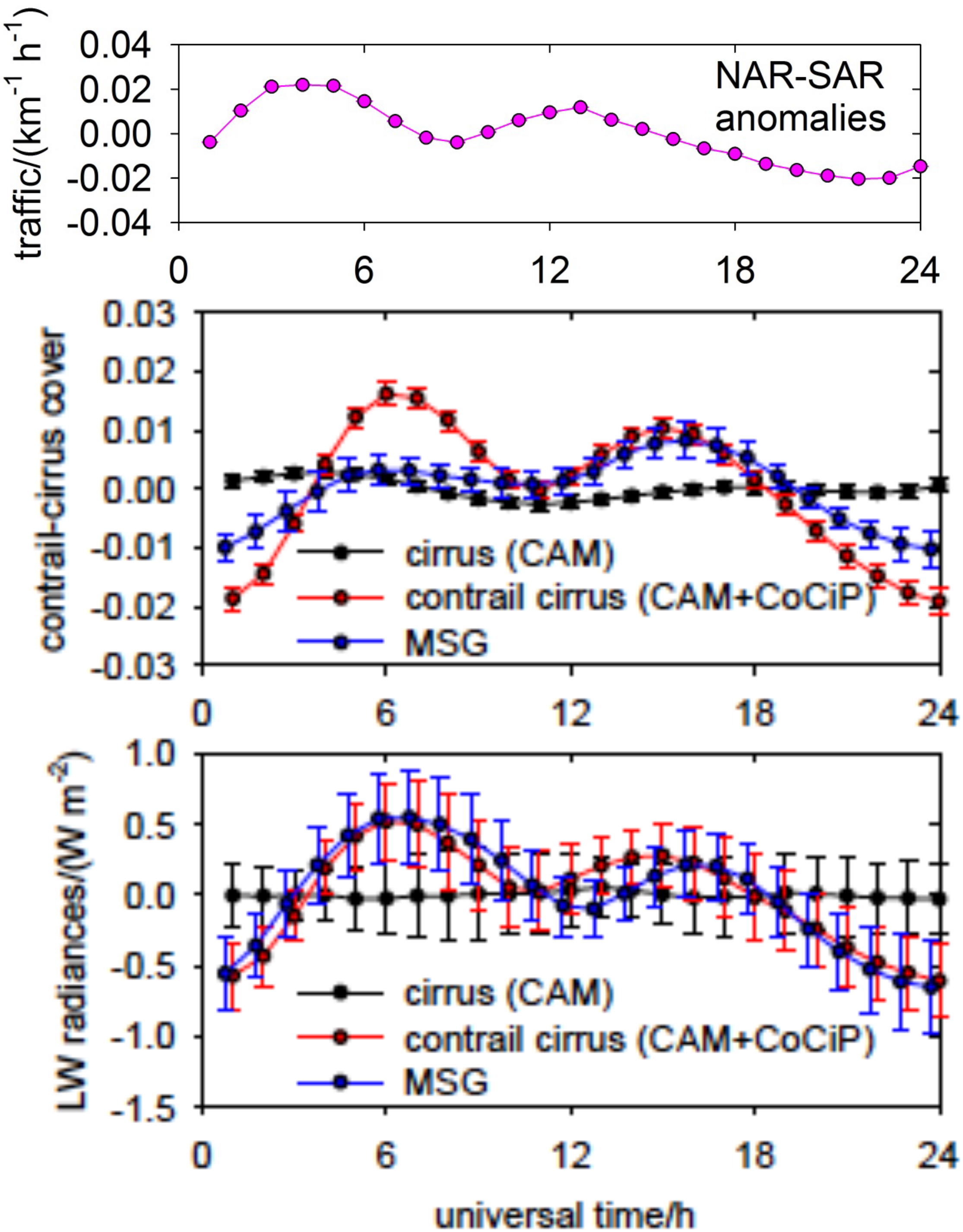

Diurnal cycle anomalies over North Atlantic

- NAR air traffic density (top)
- Meteosat (MSG) anomalies in cirrus cover and Long-wave radiation

Contrail parameter changes from humidity exchange: Range: -39 % to + 5 %. Net RF reduced by 14 %

mean values from 30 years run1 and run0 Parameter	Reference	Coupled	σ	Rel. diff/%
Flight fraction with contrail formation	0.158	0.154	0.001	-3
Flight fraction in ice supersaturated air	0.074	0.068	0.001	-8
Number of contrails at a time	2926	2862	53	-2
Relative humidity over ice at contrail formation (%)	119	116	0.5	-4
Contrail optical depth tau in solar range	0.335	0.289	0.002	-14
Cover by contrails with tau>0.1 (%)	0.551	0.505	0.007	-8
Age of contrails, length-weighted (h)	1.9	2.0	0.01	5
Contrail width (km)	17.9	18.0	0.13	1
Ice crystals in contrails (10^{12} m^{-1})	2.72	2.87	0.02	5
Ice particle number concentration (cm^{-3})	0.388	0.438	0.003	13
Ice water content (mg m^{-3})	10.6	7.5	0.05	-29
Effective radius (µm)	45.4	35.1	0.17	-23
Contrail radiative forcing, longwave, RFLW (W m^{-2})	0.171	0.143	0.002	-16
Contrail radiative forcing, shortwave, RFSW (W m^{-2})	-0.096	-0.080	0.002	-17
Contrail radiative forcing, net, RFSW+RFLW (W m^{-2})	0.074	0.063	0.001	-14
Contrail RF in North Atlantic region (NAR), (W m^{-2})	1.05	0.88	0.06	-16
Total H_2O mass inventory (Tg)	41.8	25.9	0.4	-38
Sedimentation distance in contrails (km)	-0.713	-0.734	0.008	3

Radiative forcing from dehydration

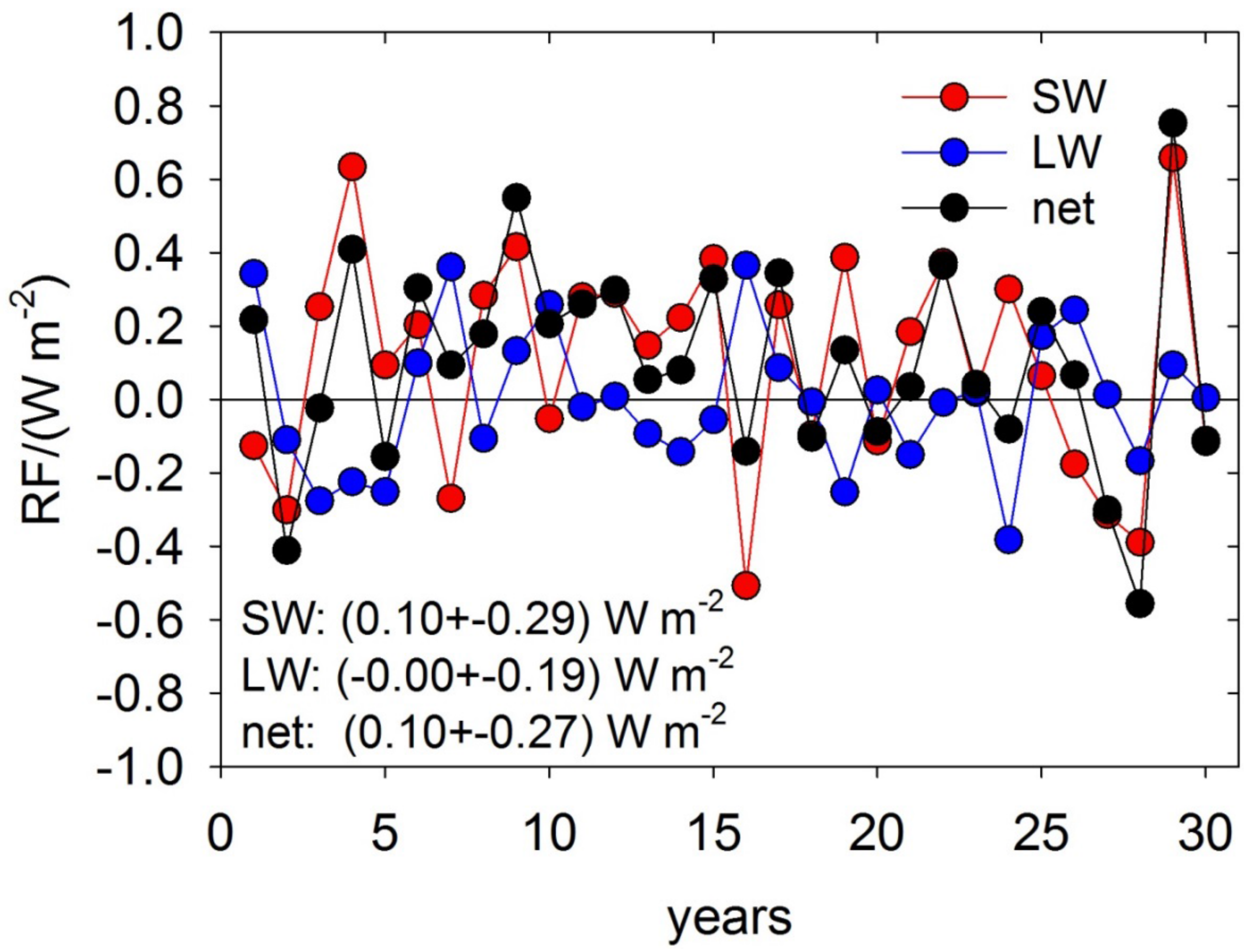

- Longwave: zero
- Shortwave: positive 0.1 ± 0.3

- Standard error:

$(\sigma/\sqrt{(n-2)}) \cong 0.05$ W/m^2

Essentially insignificant

CAM RF fluctuations mainly caused by low level cloud changes

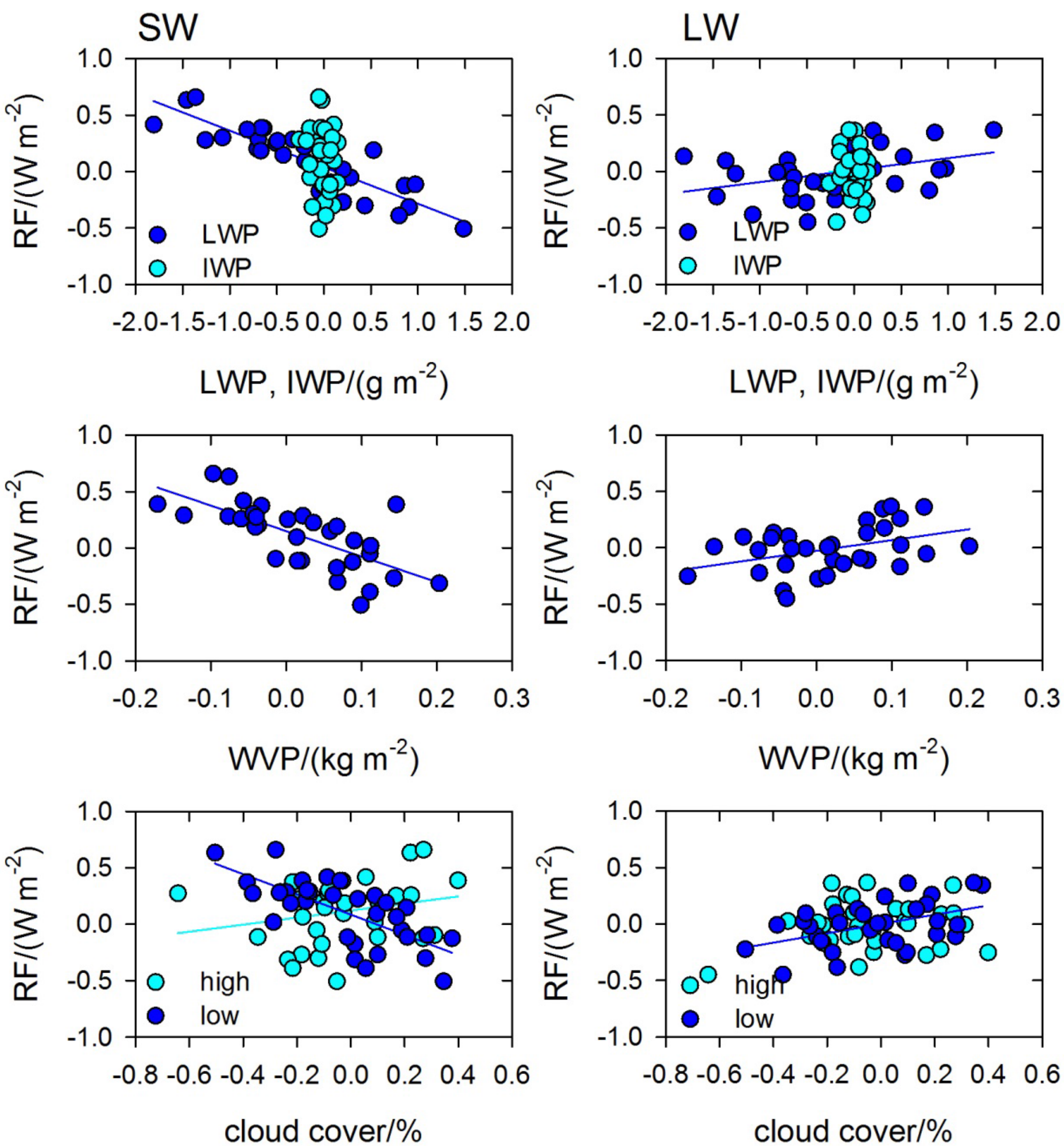

- Each point: annual mean from Run 1 – Run 0
- SW and LW radiative flux (RF) vs water path (liquid, ice, vapor) and low/high level cloud cover
- Note: Strong SW RF response to low-level cloud cover

Profiles of relative change in absolute humidity versus pressure altitude with standard errors

- 20 and 30 years mean run 1- run0 differences in Northern midlatitudes, (30°N-70°N) and global

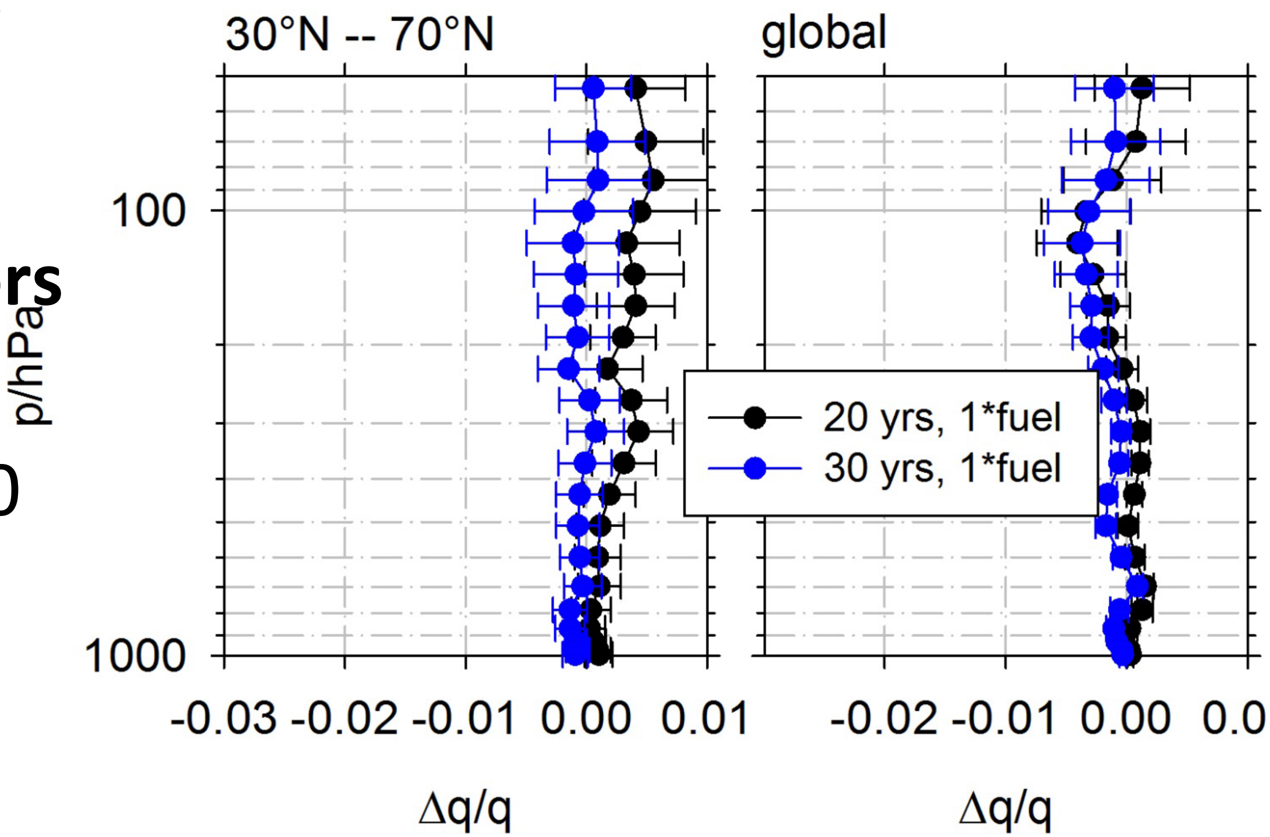

1×fuel: not significant

For 100 times enhanced soot/H2O emissions, 10 times larger water exchange CA

Max = 2.E-5 /month

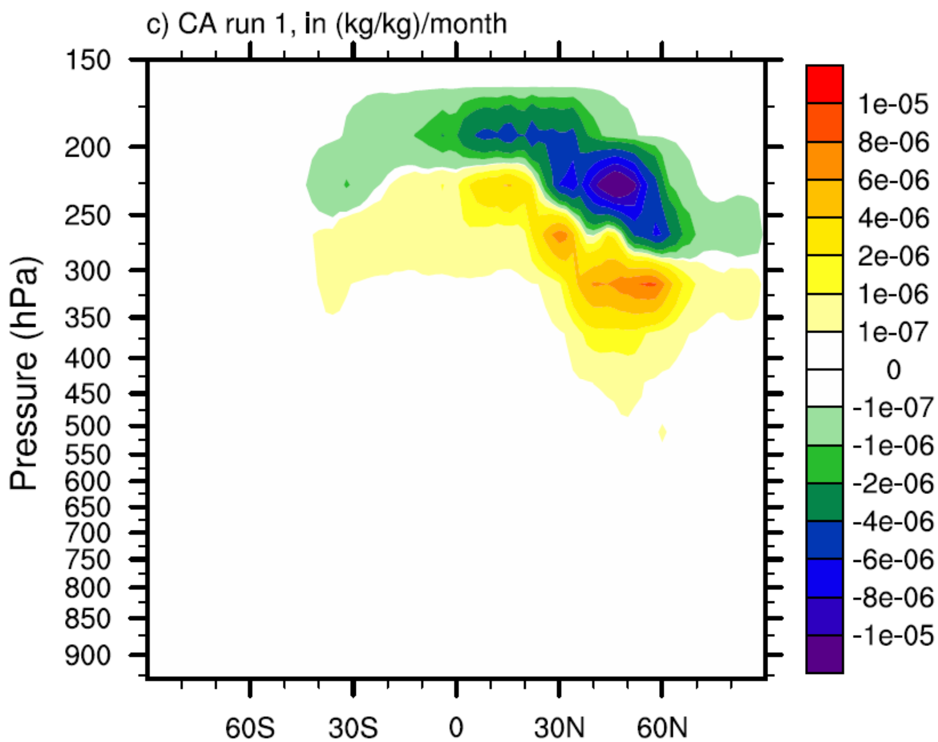

Run 1: nominal fuel consumption

Max = 2.E-4 /month

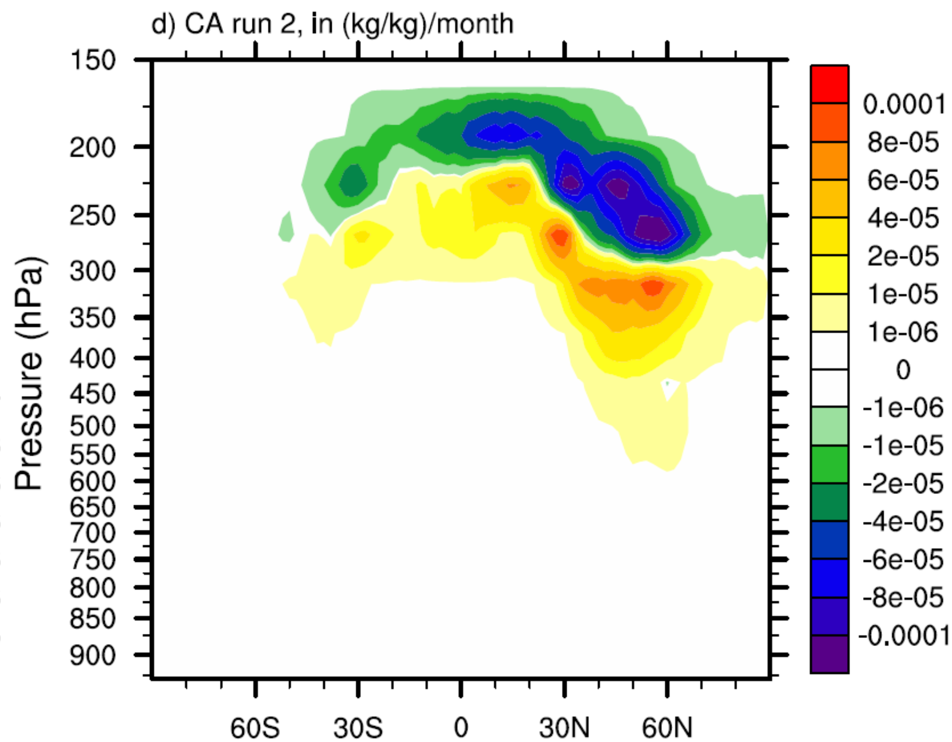

Run 2: 100 × fuel consumption

Profiles of relative change in humidity vs pressure with standard errors

- Red: Run 2 – Run 0

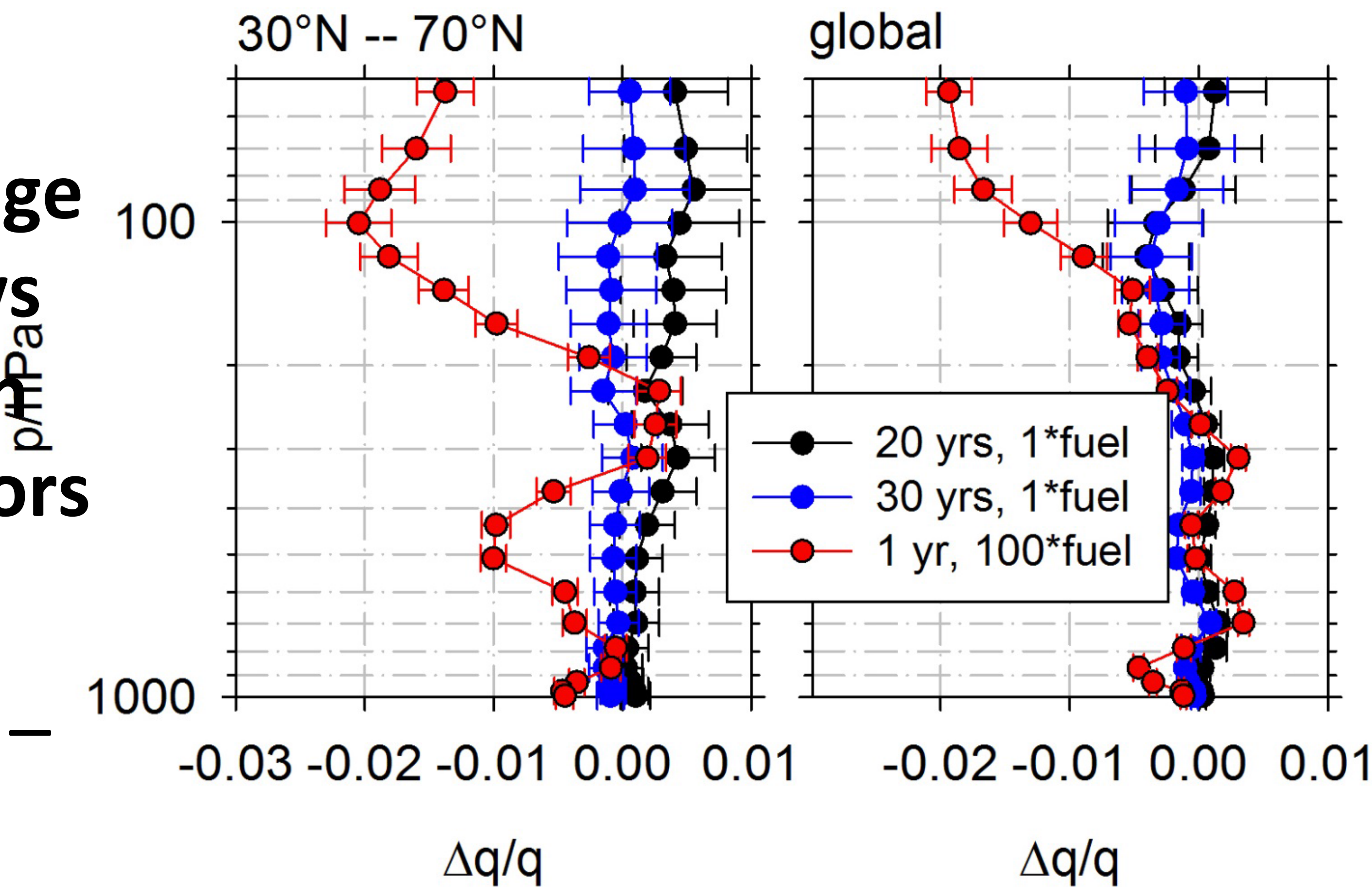

1×CA: not significant
10×CA: globally reduced RHi
+ dehydration at flight levels
+ local humidity increase in mid troposphere

Dehydration impact on global mean CAM properties

Abbreviation	Parameter	Normal mean	Normal ±σ	100×fuel mean	100×fuel ±σ	Unit
FSNT	SW net RF	0.077	0.301	0.272	0.190	$W\ m^{-2}$
FLNT	LW net RF	-0.007	0.181	-0.449	0.130	$W\ m^{-2}$
SWCF	SW cloud forcing	0.076	0.320	0.313	0.204	$W\ m^{-2}$
LWCF	LW cloud forcing	-0.017	0.132	-0.211	0.094	$W\ m^{-2}$
FSNTC	SW clear sky forcing	0.002	0.092	-0.042	0.062	$W\ m^{-2}$
FLNTC	LW clear sky forcing	0.010	0.112	-0.239	0.081	$W\ m^{-2}$
LWP	liquid water path	-0.201	0.778	-0.494	0.526	$g\ m^{-2}$
IWP	ice water path	-0.001	0.096	-0.186	0.071	$g\ m^{-2}$
WVP	water vapor path	0.011	0.086	-0.040	0.067	$kg\ m^{-2}$
CLDHGH	high-level cloud cover	-0.033	0.201	-0.642	0.103	%
CLDMED	mid-level cloud clover	-0.037	0.150	-0.241	0.123	%
CLDLOW	low-level cloud cover	-0.024	0.201	-0.365	0.131	%

changes are significant for 10 x CA, typically 10 times larger magnitude.

Dehydration reduces WVP and causes changes in low cloud properties.

Hence dehydration from sedimenting contrails impacts entire hydrological cycle.

Significant RF from dehydration (in addition to contrail RF) for 100 times increased traffic emissions

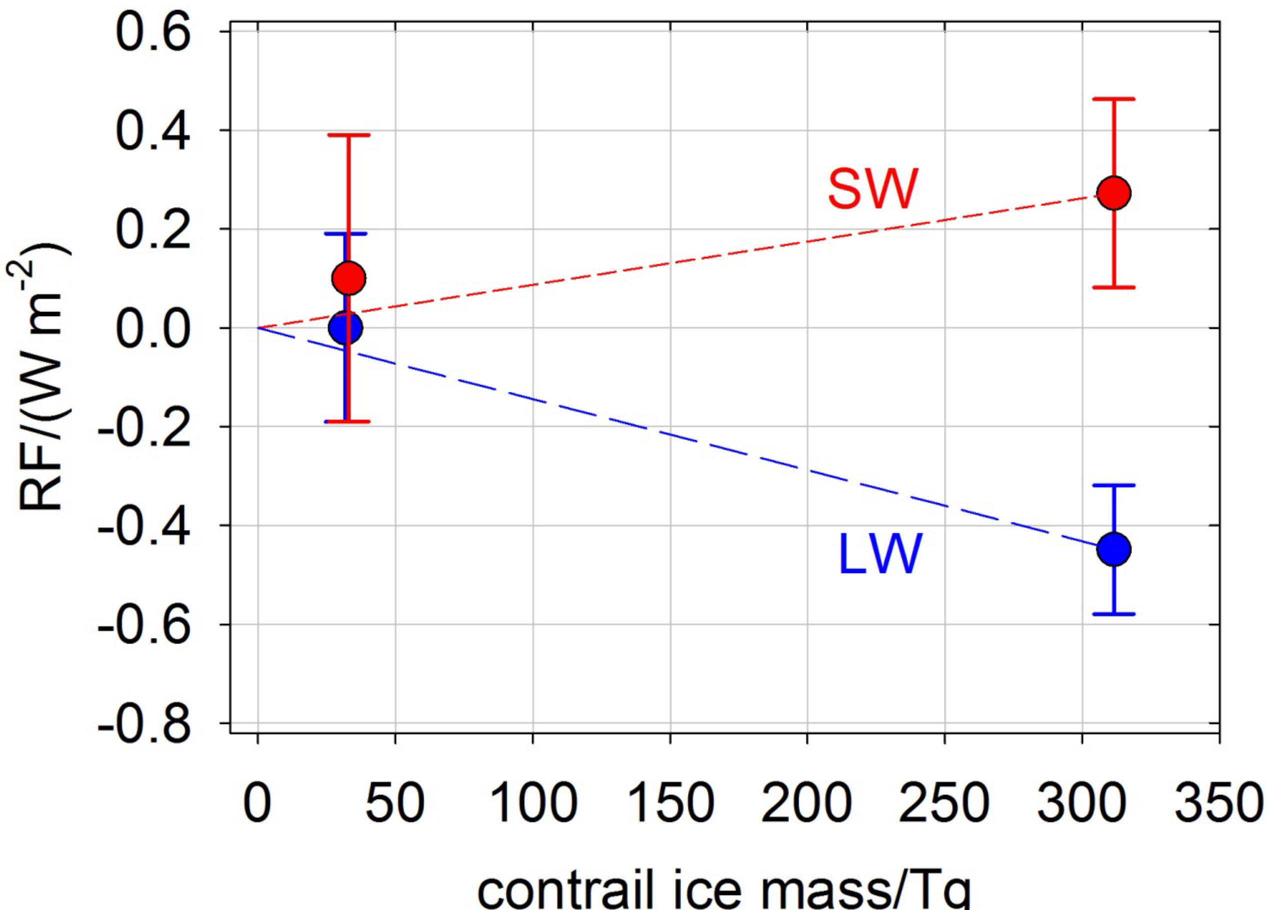

Interpolating linearly in contrail ice mass (Water exchange) suggests a RF from dehydration of order ± 0.04 (net -0.01) W m-2 for normal traffic

Radiative forcing from contrail cirrus

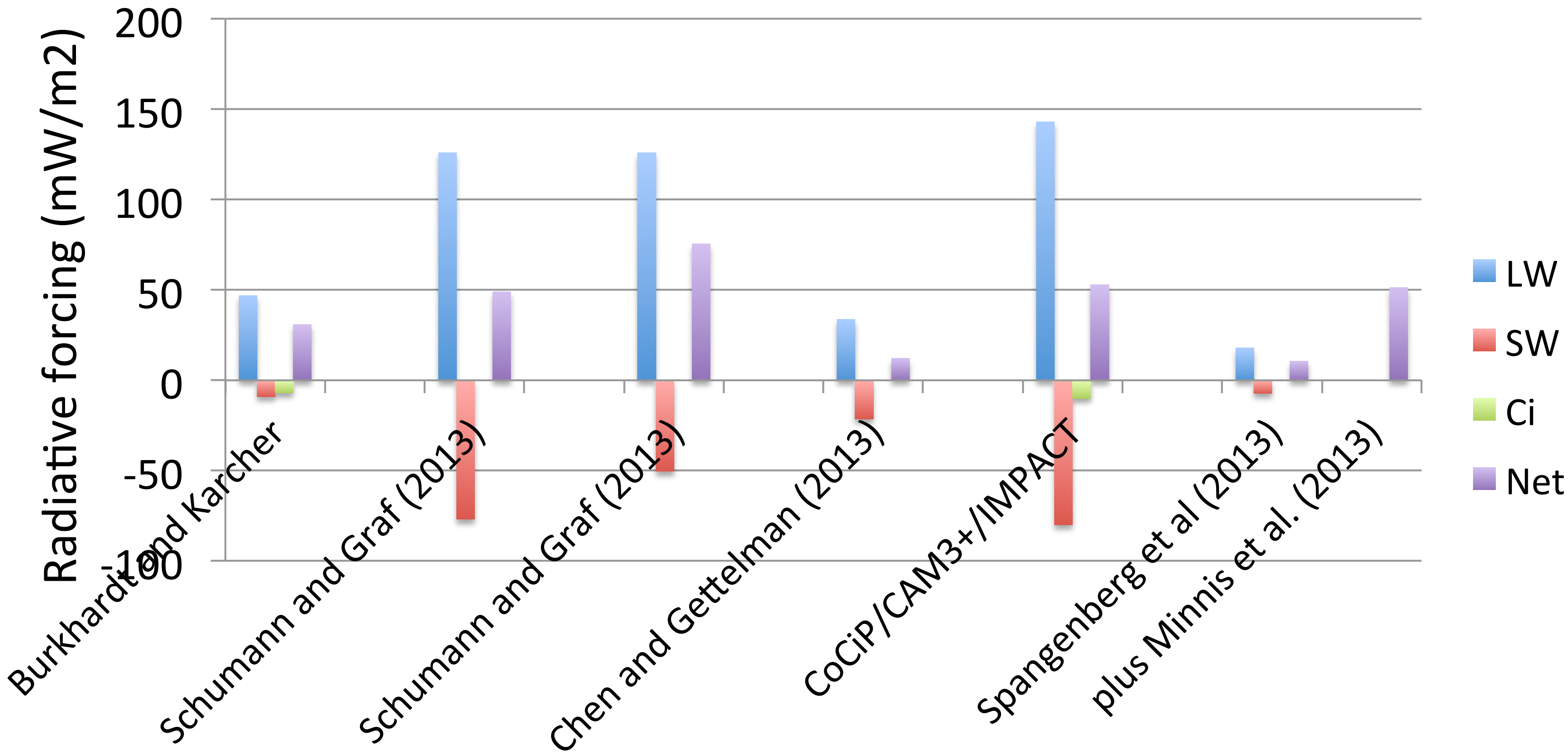

Aircraft soot effects on large-scale cirrus: -350 mW/m^2 to 90 mW/m^2 (Zhou and Penner, 2014)

Dehydration effects from contrails: Conclusions

- CoCiP/CAM contrail compare generally well with theoretical concepts. The effective time-integrated contrail area is related to ice particle sedimentation.
- Optical depth values agrees with lidar observations from space.
- The diurnal cycle of cirrus properties in the North Atlantic reflects traffic in as observed by satellites.
- Contrail water content is ~1-10^7 times larger than the amount of H_2O emitted, depending on age and RHi.
- Contrail growth -> dehydration at flight levels, large ice particles sediment, ~ 700 m, eventually sublimate and hydrate the atmosphere at lower levels.
- The drying at flight levels changes contrail properties by +5 to -30 %: Thinner contrails with larger mean age.
- Net contrail RF reduced by ~15 % from ~0.07 to ~0.06 W m^{-2}.
- Scaling with contrail ice mass (exchange) -> positive SW and negative LW RF of order $\pm$0.04 W m^{-2}, net -0.01 W m^{-2}.
- Total unchanged compared to Schumann and Graf (2013)
- Dehydration impacts entire hydrological system.